

# Studies on the Structural Dependence of Melting Behavior of Poly(ethylene terephthalate) by Differential Scanning Calorimetry

M. V. S. RAO,\* RAJ KUMAR,† and N. E. DWELTZ, *Ahmedabad Textile Industry's Research Association, Ahmedabad, 380 015, India*

## Synopsis

Thermal analysis has been carried out on polyester (PET) fibers after subjecting them to different physical modifications, such as drawing and heat setting. The relationship between structure and the various thermal transitions observed in the thermograms of poly(ethylene terephthalate) has been examined. It has been shown that the endothermic transition near the glass transition region and the exothermic transition at about 140°C, observed for amorphous PET fibers, may be associated with mesomorphic phase changes. The premelting endotherm is sensitive to the orientation, crystallite size distribution, and thermal prehistory. This transition actually represents melting of smaller crystals and recrystallization into larger crystals. Heat of fusion does not always necessarily represent the actual crystallinity, or order of the fiber prior to differential scanning calorimetry and may be influenced by several factors. The fusion curves give more information regarding crystallite size distribution than crystallinity.

## INTRODUCTION

The thermal behavior of polymers is known to be characteristic of their process history and structural organization. Thermal analysis literature concerning polyester (PET) fiber is considerably more extensive than that of other fibers.<sup>1-3</sup> There is considerable ambiguity in the interpretation of the multiple melting behavior observed in PET and other synthetic polymers.

Thermal analysis curves of PET generally consist of an endothermic transition at about the glass transition, an exothermic transition at about 140°C and a premelting endothermic transition along with a final melting transition about the melting temperature. All these transitions are shown to be processing and environment dependent.<sup>4-11</sup> A wide range of views exist regarding the nature and origin of these thermal transitions. The endothermic transition near the glass transition ( $T_g$ ) was previously ascribed to a superheating associated with glass<sup>12</sup> and now to a first-order transition<sup>13-15</sup> probably associated with a paracrystalline ordering.<sup>14</sup> Hagege<sup>6</sup> proposed that this endothermic transition may result from the fusion of a mesomorphic (nematic) phase for nonfibrous amorphous PET. Ito et al.<sup>16</sup> observed

\* Present Address: Manmade Textile Research Association, Ring Road, Surat-395 002, India.

† Chemical Physics Department, IPCL Research Centre, P.O. Petrochemicals, Vadodara-391 346, India.

that this endothermic transition is associated with a metastable molecular ordering. There are others who ascribe this transition to oriented tie-molecules in the noncrystalline matrix of the polymer.<sup>17</sup>

Multiple melting or occurrence of a premelting transition in polymers was ascribed to disorientation and melting of oriented crystals,<sup>18</sup> melting of crystals differing in size and perfection,<sup>19-22</sup> melting of different morphological forms<sup>23-26</sup> and a partial melting and recrystallization during the DSC.<sup>27-50</sup> Recently, it was shown that mechanical strains can remove or produce the multiple endotherms.<sup>51,52</sup> Rebenfeld and co-workers<sup>53</sup> showed that a hot water washing after a solvent (DMF) treatment of PET fiber can produce a characteristic premelting endotherm which is not found in the case of unwashed samples. It was also observed that for sufficiently high draw ratios, preheat-treated fibers do not show a premelting endotherm. Berndt and Bosamann<sup>42</sup> also showed that an additional premelting endotherm occurs in the case of preheated dyed polyester fibers at a temperature characteristic of the dyeing temperature. One may conclude from these observations that multiple melting endotherms in the thermograms of different polymers might have arisen from structures differing in thermal and mechanical stability. Understanding the relationship between these multiple transitions and their structural causes will have far-reaching implications in the context of fiber processing and end uses.

In this study, differential scanning calorimetry (DSC) results are supplemented by structural data obtained from X-ray diffraction and density measurement with a hope that the total knowledge will provide a better understanding of the dependence of the melting behavior of PET on its structure—modifications affected by various processing conditions, such as drawing, heat setting, etc.

## EXPERIMENTAL

**Materials** Amorphous (as-spun) polyester has been cold drawn (at room temperature) slowly to various extensions. These undrawn and cold-drawn fibers were heat set in an inert (N<sub>2</sub>) atmosphere at 200°C for 5 minutes. Another set of samples was prepared from commercially (hot) drawn polyester filaments by heat setting them at various temperatures ranging from 150 to 230°C, for 5 minutes. All the samples were quenched rapidly back to room temperature after heat setting. Heat setting was carried out in all the cases, both while holding the filament under tension so as not to allow any shrinkage and also while completely slack so that filaments shrank freely.

**Differential Scanning Calorimetry** A Perkin Elmer DSC, Model-2C was employed to record the thermograms. Since the thermograms are known to be sensitive to the experimental variables, such as the sample mass and heating rate, optimum values of these variables were initially determined using different combinations of sample sizes and scanning rates. The sample size was finally fixed at 5 mg in all cases.

Figure 1 shows the effect of heating rate on the thermograms of amorphous (as-spun) undrawn polyester filaments used in this study. A fast scanning rate of 40°C/min appeared to give better sensitivity, in particular with re-

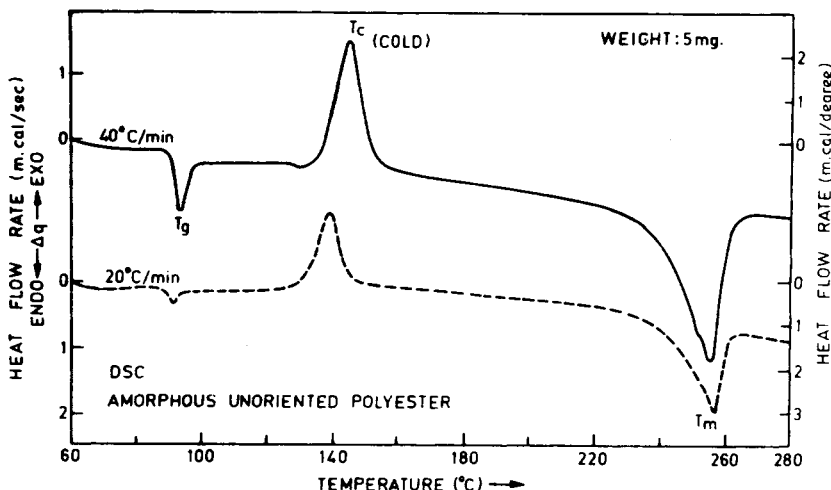


Fig. 1. DSC thermograms of as-spun, low amorphous PET recorded at two different heating rates.

gard to the glass transition and exothermic transition. The scanning rate was therefore fixed at 40°C/min in all cases. A chart speed of 12 in./min and a range sensitivity of 10 m.cal/s were employed. Indium standard was used for calibration, as well as for calculation of heat of fusion from the fusion curves. The cut fiber samples were accurately weighed (5 mg) using a "Metler" balance and placed in aluminium pans which were then crimped prior to introduction into the sample holder of the DSC.

## RESULTS AND DISCUSSION

### Thermal Analysis of Cold-Drawn Filaments

Effect of cold drawing at room temperature on the thermal behavior of amorphous (as-spun) polyester filaments is shown in Figure 2. The thermogram of the undrawn fiber shows, with increasing temperature a clear glass transition with an endothermic transition superimposed on it, an exothermic transition at about 140°C, and finally a broad melting endotherm at 257°C. With increasing drawing extension, both the endothermic peak at the glass transition temperature and the exothermic peak at 140°C tend to diminish in amplitude (height) and the glass transition becomes ill defined. At about a drawing extension of 200% both the endothermic and exothermic peaks almost disappear. The same is observed<sup>8</sup> in the case of POY (partially oriented yarns) of PET spun at different spinning rates. Above a particular spinning speed, both these endothermic and exothermic transitions are observed to disappear. This was also reported<sup>14</sup> to occur when the undrawn amorphous fibers are previously heat set at about 140°C at which the exotherm in the DSC thermogram appears. The structural causes of these two (i.e., endothermic and exothermic) transitions can be better understood by combining the observations concerning the effect of drawing on the mechanical behavior, density and X-ray diffraction patterns. The

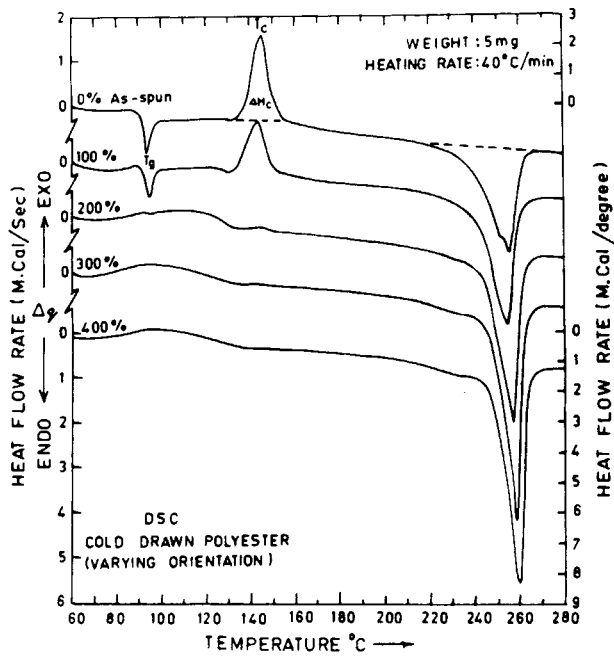


Fig. 2. Thermograms of fibers cold drawn to different extensions.

stress-strain curve of the unoriented amorphous (as-spun) PET filament is given in Figure 3. After an initial steep slope (region OA) the stress-strain curve shows a plateau (AB), after the first yield point (at 5% elongation), which indicates very high elongation of the material with little or no change in applied stress. At about point B a sudden rise in stress occurs and after the second yield point C the stress increases almost linearly with increasing strain which is indicative of a final reinforcement and stiffening of the material. X-ray diffraction patterns taken for extensions falling both in the plateau (AB) region and in the linearly increasing stress region (CD) are

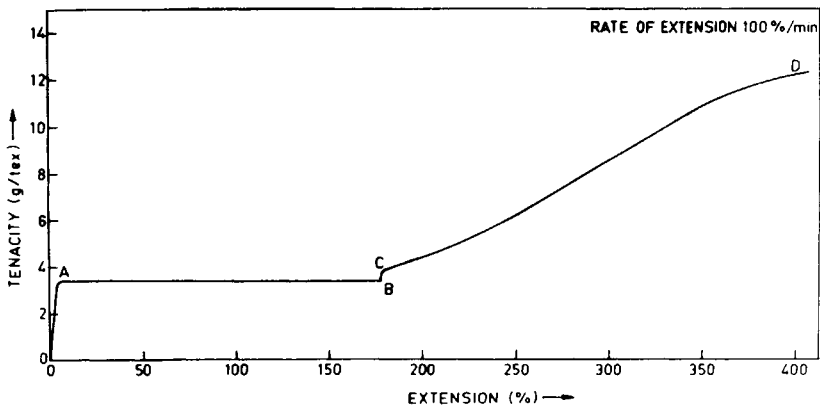


Fig. 3. Stress-strain curve (Instron G. L. = 5 cm, rate of extension 100%/min) of undrawn as-spun tow PET filament.<sup>54</sup>

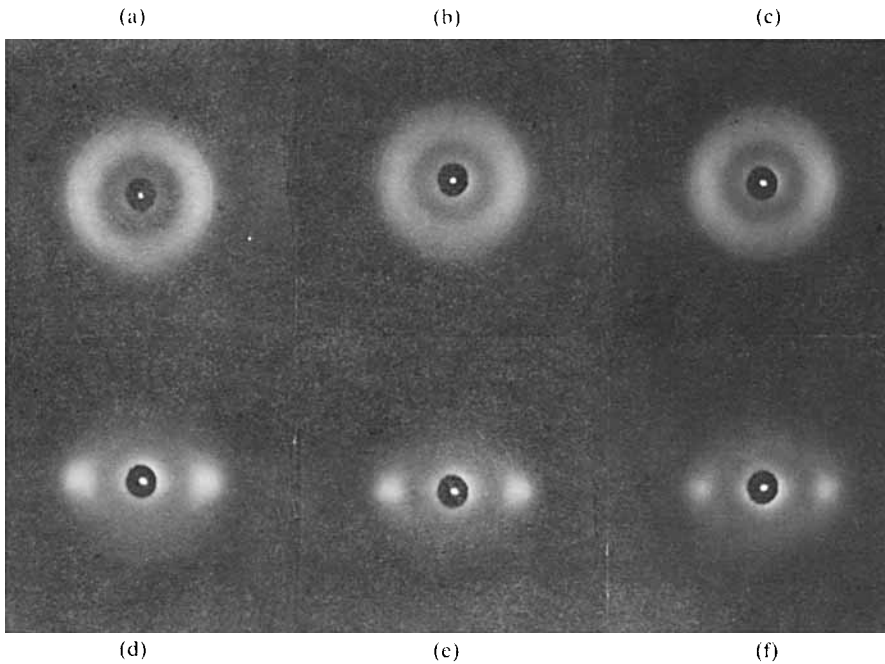


Fig. 4. X-ray diffraction patterns (CuK $\alpha$  Ni-filtered cylindrical camera, R = 3 cm) of fibers<sup>54</sup> cold drawn to different extension (a) tow, as-spun, 0%, (b) 100%, (c) 200%, (d) 300%, (e) 350%, (f) 400%.

shown in Figures 4(a) to (f). It can be noted from these that for 100% elongation which falls in the region AB and for 200% elongation falling just above the second yield point C, the diffraction patterns do not show any appreciable changes. This means that long-range order is absent for filament extensions falling just below and just above the second yield point of the stress-strain curve. Density also shows noticeable changes only above a drawing extension of 200% (Fig. 5). Hence, it cannot be concluded that the stress-induced crystallization can be the cause for the sudden increase in the mechanical stability of the filaments observed at about extensions of 180% (Point B in stress-strain curve). Molecular orientation also cannot be the cause of this sudden improvement in mechanical stability of the material because molecular orientation is observed<sup>54</sup> to increase monotonously from small extensions falling in the region AB to high extensions falling in the region CD without any discontinuous changes at any given extension. It has also been observed by us<sup>34</sup> that the dye uptake also shows a sudden decrease at about the same drawing extension at which the mechanical behavior showed sudden improvement. Considering all these observations together, the simultaneous disappearance of both the near glass transition endothermic peak and exothermic transition at about 104°C by drawing above 200% elongation can be ascribed to the formation of a thermodynamically stable structure<sup>55</sup> when the sample is heated above its glass transition temperature during the DSC. The structure formed must also be mechanically stable and resist deformation while its formation should not involve any change in X-ray diffraction patterns and density. It is observed by

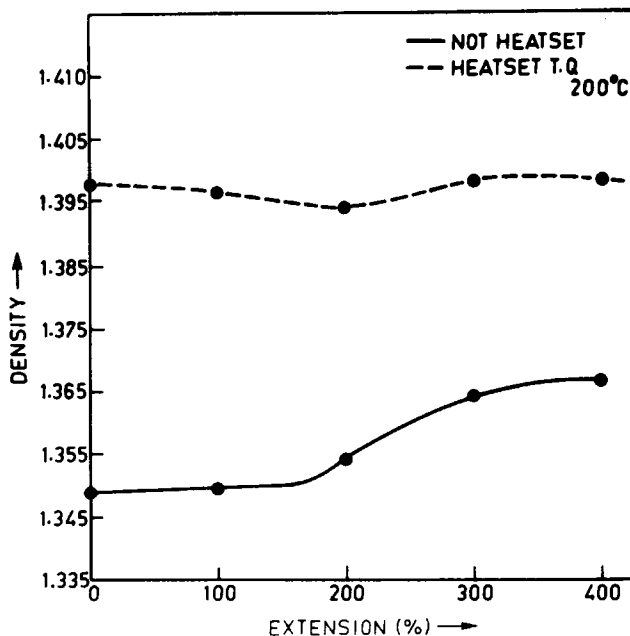


Fig. 5. Density (vs.) drawing extension (%) for cold-drawn and tension heat-set (200%) PET samples.<sup>54</sup>

Stuart<sup>56</sup> that short-range order, or small crystallites with an edge length of  $10\text{\AA}$ , cannot be detected by X-ray diffraction methods. Hearle<sup>55</sup> was the first to argue in favor of the existence of short-range order in rapidly quenched melts of polymers based on thermodynamics principles. Hence, it is possible that a mesomorphic order may exist in the rapidly quenched, as-spun PET filaments, the extent of which is dependent on the spinning and cooling conditions. It is suggested here that this mesophase or paracrystalline order may preferably be "nematic" because the material is still extensible, by heating up to the glass transition temperature, these nematic crystals should melt which is a prerequisite for the free thermal motion of the molecules. This would result in the appearance of an endothermic transition at  $T_g$ .

When the heating is continued up to  $140^\circ\text{C}$  due to the onset of rotations of rigid aromatic (terephthalate segments) a more thermodynamically stable mesophase, but yet another paracrystalline state of order, namely, the "smectic" type results. Figure 6 shows a schematic diagram of these two types of paracrystalline order. This isomerization lowers the entropy of the system and results in an exothermic transition. From Figure 6 it can also be seen that smectic structures are less easily deformable<sup>14</sup> and therefore mechanically more stable.

By the application of orientating stress (drawing) the easily deformable nematic phase is gradually converted into the less deformable smectic phase which will be almost complete after a drawing extension of about 200%. Below this extension both the nematic and smectic forms coexist simultaneously, while above this extension only the smectic form exists. This explains why the endothermic transition at  $T_g$  and the exothermic transition

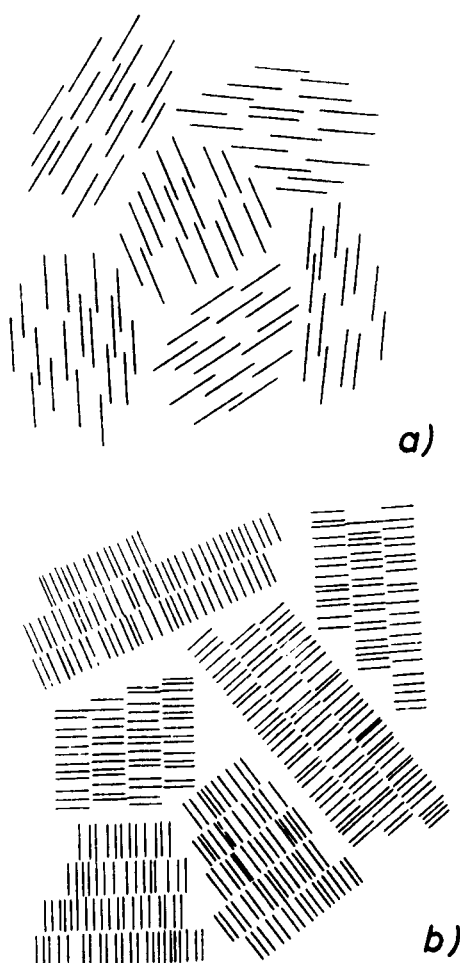


Fig. 6. Schematic diagram showing different types of paracrystalline order<sup>14</sup> (a) nematic and (b) smectic.

at 140°C gradually diminish with increasing drawing extension and finally disappear at about 200% drawing extension. The experimental evidence<sup>57</sup> and theoretical reasoning<sup>58</sup> have already been given for the existence of these mesophases in the so-called amorphous polymers.

### Thermal Analysis of Drawn and Heat-Set Filaments

Double melting phenomenon is observed in the thermograms of both undrawn and drawn heat-set filaments. While a premelting endotherm for undrawn fibers (Fig. 7) is observed at the same temperature as that of the pretreatment temperature, for drawn fibers (Fig. 8), its position and area seem to depend upon the drawing extension (orientation). In the latter case, this premelting endotherm progressively shifts to higher temperatures, much above that of the pretreatment temperature (200°C), with increasing drawing extension. The area under the peak also gradually diminishes as the

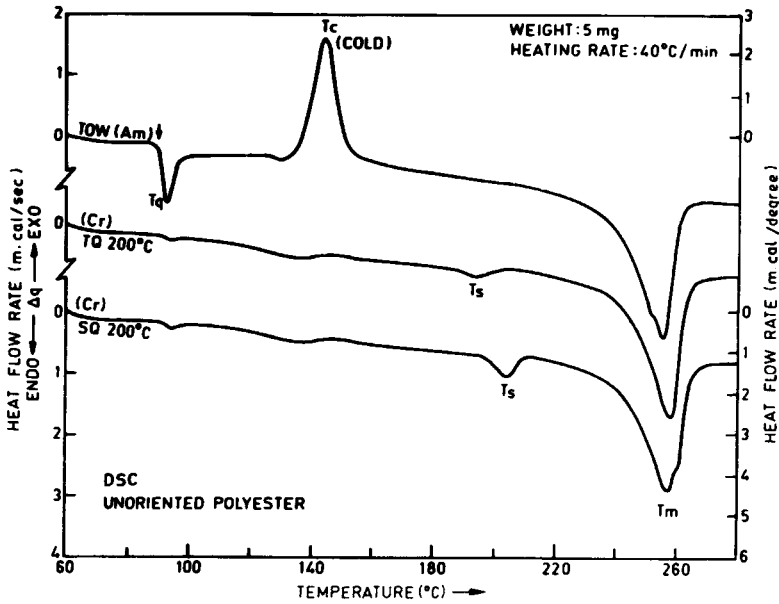


Fig. 7. Thermograms of PET fibers undrawn tow and thermal treated at 200°C under tension (TQ) and slack (SQ).

drawing extension increases and the peak finally disappears at very high drawing extension. A progressive increase in the crystallite orientation in these drawn and heat-set filaments is evident from their X-ray diffraction patterns shown in Figures 9(a) to (f).

For commercial drawn polyester filaments (draw ratio 4.25 x and drawing temperature 80°C), this premelting endotherm appears at a temperature

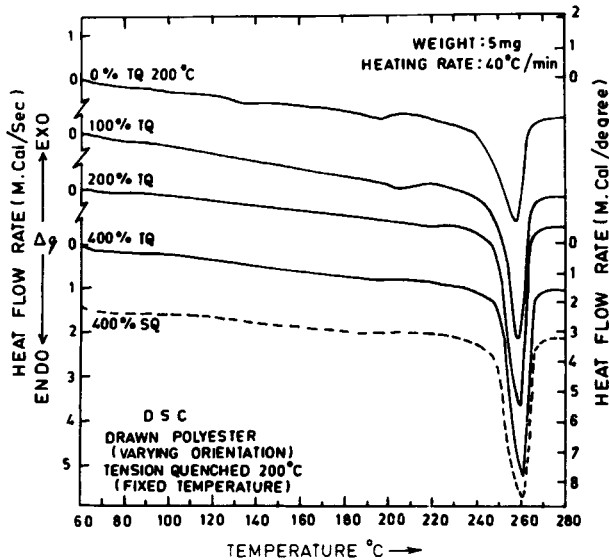


Fig. 8. Thermograms of PET fibers cold drawn to different extensions (%) and heat set under tension at 200°C.



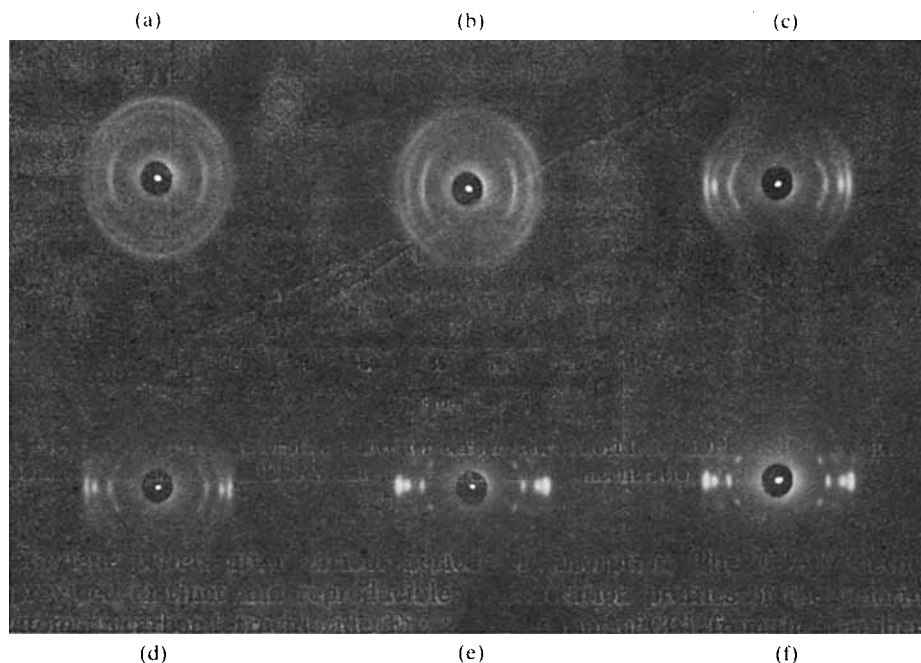


Fig. 9. X-ray diffraction patterns of fibers as in Figure 4 but after tension heat setting at 200°C.

nearly 20°C above the setting temperature for all different setting temperatures as shown in Figure 10. The area under this endotherm shows negligible dependence on the setting temperature, while the area under the main melting peak ( $T_m$ ) increases with increasing setting temperature. The area under the main melting peak is also shown (Fig. 8) to increase with increasing drawing extension. There are two different observations often found in literature regarding the mutual relationship of the premelting and main-melting endotherms. In one case,<sup>41,42,52</sup> similar to the present observations, no mutual relationship in positions of peaks and areas under these two peaks have been observed. While in the other<sup>4,24,25,31,32,48,53,55</sup> there is a definite mutual reciprocal relationship noted between the position of and areas under, the premelting and main-melting peaks. However, the difference in these two cases lies in the range of temperatures and time employed during pretreatment of the samples. When the annealing temperatures are very high, close to the melting temperature, and for very long annealing times, a mutual reciprocal relationship between these two peak positions and areas does exist. When the annealing or pretreatment temperatures are low and the time of treatment short, as is the case in normal industrial practice there is no mutual relationship between these two peak positions and areas<sup>29</sup> and the position of the premelting endotherm is truly characteristic of the pretreatment temperature alone.

Hence, from the observation that the area under and position of the peak are dependent on sample orientation history (drawing extension) and thermal history (heat-setting temperature) it is more appropriate to explain the

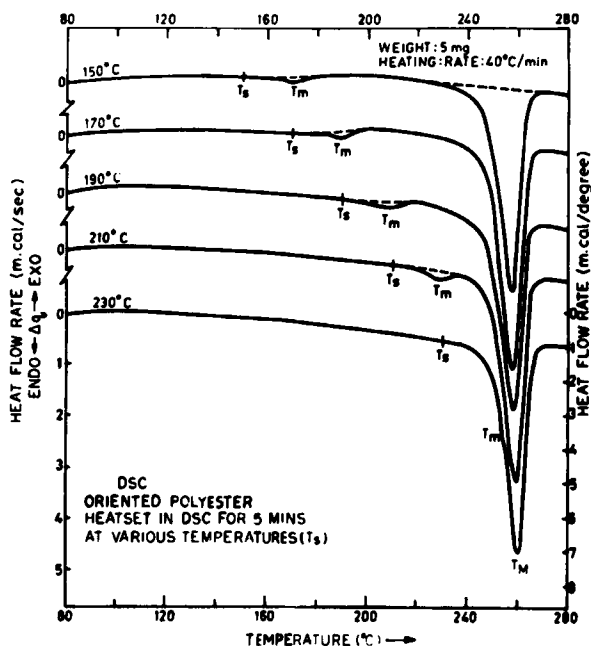


Fig. 10. Thermograms of commercial PET (hot) drawn filaments heat set at different temperatures.

occurrence of the premelting endotherm as due to the melting of small and imperfect crystals with a broad crystallite size distribution followed by the growth of large and more perfect crystals with a narrow distribution of crystallite dimensions. The dependence of the premelting peak position and its area on sample orientation (drawing extensions) is a direct consequence of the entropy restrictions<sup>51</sup> on melting crystals due to the increased frozen-in stresses in the noncrystalline regions. For very high orientations all crystals melt within the main melting range<sup>53</sup> and therefore no premelting endotherm should occur.

### Heats of Fusion

Heats of fusion are generally considered as measures of crystallinity in polymers. A comparison of the dependence of heat of fusion on preorientation and prethermal history with the corresponding crystallinity data from X-ray diffraction and density data lead us to believe that the heats of fusion represent closely the crystallinities within the sample only when orientation prehistory is the same for all of them.

When the draw ratio is fixed, such as the case with the commercial sample (4.25x) the heats of fusion varied with the setting temperature (Fig. 11) in a similar way to the crystallinities measured from X-ray diffraction and density data.<sup>54</sup> In samples with different orientations (drawing extensions), although the heats of fusion (Fig. 12) vary in a similar way as the density values (Fig. 5), it should be noted that drawn heat-set filaments show higher heats of fusion than those of the untreated drawn filaments, whereas the reverse is true with the density values and crystallinities as measured by

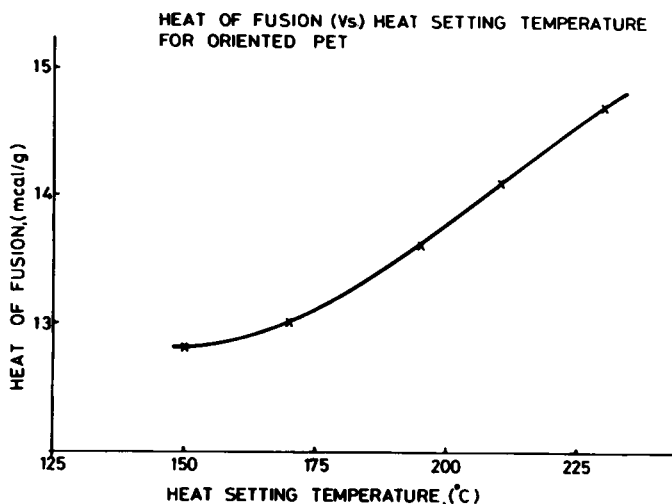


Fig. 11. Heat of fusion (vs.) heat-setting temperature.

X-ray diffraction methods.<sup>54</sup> It was also noted that the drawn heat-set samples have higher crystallinity than the drawn untreated samples. This discrepancy is easily explained, based on the fact that the fusion curve represents the structural state of the material after it is subjected to a programmed heating during the DSC. If the initial structure is noncrystalline but oriented, such as the case with the cold drawn but untreated filaments, considerable reorganization of the structure takes place during DSC and the fusion curve represents only this reorganized structural state rather than the initial one. For previously heat-set fibers, which are crystalline to some extent, the high thermal stability of the structures resist reorganization for most of the DSC heating program and the final melting curve more or less represents the initial structural state prior to DSC.

It is also noted that the heat of fusion of undrawn heat-set filaments are lower than those of drawn heat-set filaments which is again contrary to the trend shown in crystallinities as measured from X-ray diffraction and den-

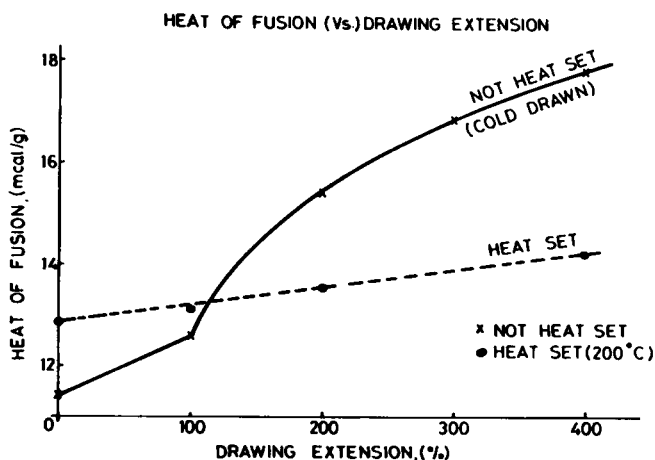


Fig. 12. Heat of fusion (vs.) drawing extension (%).

sity data.<sup>54</sup> The crystallinities measured by X-ray diffraction and density data are always higher for the undrawn heat-set filaments compared to those of drawn heat-set filaments. An explanation for this is that the fusion curves are sensitive to the crystallite orientation and size distribution which will largely influence the area under the fusion curve.

Crystallite size distribution in the undrawn heat-set and drawn heat-set fibers has been examined using X-ray equatorial diffraction measurements.<sup>54</sup> It has been noted that the heat-set undrawn fibers are highly crystalline but have a very broad distribution of small crystals, while the heat-set drawn fibers are comparatively less crystalline but have a very narrow distribution of large crystals. This is exactly reflected in the fusion curves in the corresponding thermograms. A broad melting range for undrawn heat-set fibers (Fig. 7) and a narrow melting range for drawn heat-set fibers (Figs. 8 and 10) can be noted from the thermograms. In the former case, melting occurs over a fairly wide range of temperatures and areas under the peak do not truly reflect the extent of crystallinity within the sample.

### SUMMARY

There is considerable experimental evidence, both from the results obtained here and reported elsewhere,<sup>6, 13-18</sup> that the endothermic transition near the glass transition temperature may be associated with the melting of a nematic type mesophase.

The premelting endotherm, appearing in the thermogram of thermally treated polyester materials, is influenced by preorientation, crystallite size, and the distribution of crystallite dimensions, and acutally represents the melting of smaller or imperfect crystals in favor of the formation of larger and more perfect crystals.

The fusion curves provide more valid information on the distribution of crystallite dimensions present, as well as average crystallite size, than on the total crystallinity content. For highly oriented crystalline polymers the heat of fusion may perhaps represent the true crystallinity.

The authors wish to thank Dr. T. Radhakrishnan, Director of ATIRA for permitting this work to be published. One of us (M. V. S. Rao) is also indebted to the Council of Scientific and Industrial Research, India, for financial assistance in the form of a Junior Research Fellowship.

### References

1. J. G. Fatou, *Differential Thermal Analysis and Thermogravimetry of Fibres*, Applied Fibres Science, F. Happey, Ed., Academic Press, London, 1979, Vol. 3, p. 23.
2. B. Wunderlich, *Determination of the History of a Solid by Thermal Analysis*, Thermal Analysis in Polymer Characterisation, E. A. Turi, Ed., Heyden and Sons, Inc., Philadelphia, 1981.
3. M. Jaffe, *Fibres*, Thermal Characterization of Polymeric Materials, E. A. Turi, Ed., Academic Press, New York, 1981, Ch. 7, p. 709.
4. G. Prati and A. Seves, *Chemiefasern/Textil Industries*, 1974, April 263.
5. G. Prati and A. Seves, *Tinetoria*, **70** (8), 267 (1973).
6. R. Hagege, *Text. Res. J.*, **47**, 229 (1977).
7. J. Shimizu, N. Okui, T. Kikutani, and K. Toriumi, *Sen-i-Gakkeishi*, **34**, 35 (1978).
8. H. M. Heuvel and R. Huisman, *J. Appl. Polym Sci.*, **22**, 2229 (1978).

9. G. Perez and C. Lecluse, *Proc. Int. Chem. Fiber Conf.*, **18**, 1 (1979).
10. R. M. Ikeda, *J. Polym. Lett. Ed.*, **18**, 325 (1980).
11. H. Springer, U. Brenkmann, and G. Hinrichsen, *Coll. Polym. Sci.* **259**, 38 (1981).
12. B. Wunderlich, D. M. Bodily, and M. H. Kaplan, *J. Appl. Phys.* **35**, 95 (1964).
13. H. D. Keith, *Kolloid Z. U. Z. Für Polymer*, **231**, 421 (1969).
14. R. Bonart, *Kolloid Z. U. Z. Für Polymer*, **231**, 438 (1969).
15. G. W. Miller, *J. Polym. Sci. Polym. Phys. Ed.*, **13**, 1031 (1975).
16. E. Ito, K. Yamamoto, Y. Kobayashi, and T. Hatakeyama, *Polymer*, **19**, 39 (1978).
17. A. Jeziorny, *J. Appl. Polym. Sci.* **28**, 1025 (1983).
18. T. R. White, *Nature*, **175**, 895 (1955).
19. T. Yoshimoto and A. Miyagi, *Kogyo Kagaku Zasshi*, **69**, 1771 (1966) (*J. Chem. Soc. Japan, Ind. Chem. Sect.* **69** 1771 (1966)).
20. H. Kanetsuna and K. Malda, *Kogyo Kagaku Zasshi*, **69**, 1788 (1966).
21. A. Seves and L. Vicini, Paper presented at the Italian group meeting of the international confederation for thermal analysis, Milan (1975).
22. A. Seves and L. Vicini, *Tintoria*, **2**, 1 (1975).
23. F. J. Hybart and L. D. Platt, *J. Appl. Polym. Sci.* **11**, 1449 (1978).
24. J. P. Bell and J. H. Dumbleton, *J. Polym. Sci. A 2*, **7**, 1033 (1969).
25. J. P. Bell and T. Murayama, *J. Polym. Sci. A 2*, **7**, 1059 (1969).
26. R. C. Roberts, *Polymer*, **10**, 117 (1969).
27. M. Jaffe and B. Wunderlich, *Kolloid Z. U. Z. Für Polymer*, **217**, 203 (1967).
28. M. Ikeda, *Kobunshi Kagaku*, **25**, 87 (1968).
29. E. Wiesen, *Faserforschung Und Textil Technik* **19**, 301 (1968).
30. D. L. Nealy, J. G. Doris, and C. J. Kilber, *J. Polym. Sci. A 2*, **8**, 2141 (1970).
31. R. C. Roberts, *J. Polym. Sci.* **B8**, 381 (1970).
32. P. J. Holdsworth and A. Turner Jones, *Polymer*, **12**, 195 (1971).
33. J. P. Bell, *Tex. Res. J.*, **42**, 292 (1972).
34. G. E. Sweet and J. P. Bell, *J. Polym. Sci.*, **A 2**; **10**, 1273 (1972).
35. A. Miyagi and B. Wunderlich, *J. Polym. Sci. A 2; **10**, 1401 (1972).*
36. G. Valk, *Lunzinger Ber.* **33**, 1 (1972).
37. S. C. Sharma *Ind. J. Chem.*, **12**, 1297 (1974).
38. G. Coppola, P. Fabbri, B. Pallesi, G. C. Alponso, G. Domdero, and E. Pedemonte, *Makromol. Chem.* **174**, 176 (1975).
39. G. Ceccorulli, F. Maneschalchi, and M. Pizzoli, *Makromol. Chem.*, **176**, 1163 (1977).
40. S. Y. Hobbs and C. F. Pratt, *Polymer*, **16**, 462 (1975).
41. W. Schauler and E. Liska, *Faser Forsch. Textiletech.*, **26**, 225 (1975).
42. H. J. Berndt and A. Bosamann, *Polymer*, **17**, 241 (1976).
43. E. Wiesner, *Chem. Valakna*, **26**, (3-4) 146 (1976).
44. G. Heidermann and H. J. Berndt, *Melliand Textilber* (English ed.) **6**, 485 (1976).
45. J. J. Oswald, E. A. Turi, P. J. Harget, and Y. P. Khanna, *J. Macromol. Sci. (Phy)*, **B 13**, (2), 231 (1977).
46. Y. W. Huh and Y. Y. Choi, *Sumyu, Konghakhoe, Chi*, **14** (2), 49 (1977).
47. R. Mcgregor, P. L. Grady, T. Montgomery, and T. Adeimy, *Text. Res. J.*, **47**, 598 (1977).
48. S. Fakirov, E. W. Fisher, R. Hoffmann, and G. F. Schmidt, *Polymer*, **18**, 1121 (1977).
49. M. C. Lang, C. Noel and A. P. Legrand, *J. Polym. Sci. Polym. Phys. Ed.*, **15**, 1319 (1977).
50. N. Oberbergh, M. Girolamo, and A. Keller *J. Polym. Sci. Poly Phys. ed.*, **15**, 1475 1485 (1977).
51. M. Todoki and T. Kawagunhi, *J. Polym. Sci. Poly. Phys. Ed.*, **15**, 1067, 1507 (1977).
52. K. Tashiro, Y. Naki, M. Kobayashi, and H. Tadokoro, *Macromolecules*, **13**, 137 (1980).
53. H. Jameel, H. D. Noether, and L. Rebenfeld, *J. Appl. Polym. Sci.*, **27**, 773 (1982).
54. M. V. S. Rao, Ph. D. thesis, Gujarat University Ahmedabad India (1982).
55. J. W. S. Hearle, *J. Appl. Polym. Sci. Poly. Symp.* **31**, 137 (1977).
56. H. A. Stuart, *Augew. Che.*, **6**, 844 (1967).
57. G. S. Y. Yeh and P. H. Geil, *J. Macromol. Sci.*, **B 1**, 251 (1967).
58. R. E. Robertson, *J. Phys. Che.*, **69**, 1575 (1965).

Received December 1, 1984

Accepted September 9, 1985